J. Phys. D: Appl. Phys. 28 (1995) 1047–1057. Printed in the UK

Continuous emission due to radiative ion–atom association and charge exchange in weakly ionized plasmas of H, He, Li and Na

A M Ermolaev†, A A Mihajlov‡, Lj M Ignjatović‡ and M S Dimitrijević§

† Department of Physics, University of Durham, Science Laboratories, Science Laboratories, Durham DH1 3LE, UK
‡ Institute of Physics, PO Box 57, 11001 Belgrade, Yugoslavia
§ Astronomical Observatory, Volgina 7, 11050 Beograd, Yugoslavia

Received 26 July 1994, in final form 13 February 1995

Abstract. The contribution of radiative charge exchange and radiative association in symmetrical ion–atom collisions to continuous EM radiation from weakly ionized gaseous plasmas has been considered within the semiclassical adiabatic theory. The differential (in λ) cross sections for spontaneous photon emission and the general expressions for the spectral coefficients of emission and absorption are given. The hydrogen and helium plasmas that are representative of two different optical types of gaseous medium have been studied in a broad range of T and λ, $4000 \leqslant T$ (K) $\leqslant 20\,000$ and $200 \leqslant \lambda$ (nm) $\leqslant 1000$. The domain of T and λ, where ion–atom collisions contribute significantly to continuous plasma spectra, has been established. The case of weakly ionized alkali metal plasmas of Li and Na has been studied in the same interval of λ but at lower temperatures, $1500 \leqslant T$ (K) $\leqslant 3500$. The relevance of the results to studies of laboratory plasmas is discussed.

1. Introduction

The ion–atom contribution to continuous EM emission from hydrogen plasmas was first estimated by Boggess (1959) who used the quasistatic approach which had been suggested earlier by Bates (1951a, b) for radiative molecular collisions. Subsequently, this contribution was discussed by several other authors including Roberts and Voigt (1971) and Ott *et al* (1973, 1975). In all these works *strongly ionized*, high-temperature plasmas were considered where electron–ion processes dominated and where the processes involving neutral atoms were relatively weak. In such plasma conditions, the contribution of ion–atom collisions to continuous emission from the plasma is negligibly small, as may be expected. The present authors have recently drawn attention to the fact that the ion–atom contribution to the continuous radiation from *weakly ionized* plasmas may not be negligible, under certain physical conditions. This is the case, for example, for the relatively low-temperature hydrogen and helium plasmas of some stellar atmospheres where the typical pressure is of order 10^{-4}–10^{-2} atm and the degree of ionization $\alpha \sim 10^{-4}$–10^{-3} (Mihajlov *et al* 1993a, 1994), and for some helium laboratory plasmas with degree of ionization 10^{-4} (Mihajlov *et al* 1993b).

In the present work we report a systematic study of emission/absorption owing to ion–atom collisions for a wide range of physical conditions typical of laboratory plasmas. The calculations have been carried out using a quasistatic model based on the semiclassical adiabatic approximation for heavy-particle collisions (Mihajlov and Popović 1981). As has recently been shown for radiative p+H collisions (Ermolaev and Mihajlov 1991), this model gives the relevant cross sections which remain close to the exact numerical solution of the semiclassical problem, at incident velocities v below 0.1–0.2 au. Therefore, the range of T where the quasistatic model is applicable extends to much higher temperatures than those which are of interest in the current study. The present formulation of the model allows one to treat symmetrical collisions $A+A^+$ for atoms A with s electrons in the outer shell. The reported calculations are for the hydrogen and helium plasmas as well as for alkali metal plasmas of Li and Na.

The present calculations of emissivities which assume the Maxwellian distribution of velocities for atomic particles, have been carried out in the optical

0022-3727/95/061047+11$19.50 © 1995 IOP Publishing Ltd

interval $200 \leqslant \lambda$ (nm) $\leqslant 1000$ for a range of constant pressures between 10^{-4} and 10 atm. For hydrogen plasma, the reported results are for a range of temperatures $4000 \leqslant T$ (K) $\leqslant 16\,000$ which includes the important interval $4000 \leqslant T$ (K) $\leqslant 8000$ that had not been considered by Roberts and Voigt (1971). For helium plasma, the range is $4000 \leqslant T$ (K) $\leqslant 20\,000$. The calculations on He have used refined data for the model which allows one to test our previous calculations (Mihajlov and Dimitrijević 1992, Mihajlov *et al* 1993a). The domain of physical conditions treated in the present work corresponds to a state of weakly ionized plasma of H and He with degree of ionization $10^{-7} \leqslant \alpha \leqslant 10^{-2}$.

For plasmas of Li and Na, the reported calculations of emission coefficients are in the range $1500 \leqslant T$ (K) $\leqslant 3500$. Apparently this is the first estimate of the ion–atom contribution to continuous emission in alkaline metal plasmas.

The comparison between ion–atom radiative collisions and electron–ion/atom radiative processes has been carried out for the hydrogen and helium plasmas which obey the Maxwellian distributions, with the same T for heavy particles and for the free electrons. However, the theory presented can be applied to non-equilibrium plasmas once the required distributions are known.

2. Radiative processes and their characteristics

2.1. Radiative collisions

The radiative processes to be considered here are radiative ion–atom photoassociation/photodissociation

$$A^+ + A \Leftrightarrow \epsilon_\lambda + A_2^+ \qquad (1a)$$

and radiative charge transfer

$$A^+ + A \Leftrightarrow \epsilon_\lambda + \begin{cases} A^+ + A \\ A + A^+ \end{cases} \qquad (1b)$$

where $\epsilon_\lambda = 2\pi\hbar c/\lambda$ is the energy of a photon with a wavelength λ and A is an atom with the optical s electron(s).

Reactions (1*a*,*b*) will be compared with the electron–ion free–bound (photorecombination/photoionization) and free–free (emission-bremsstrahlung/absorption) transitions

$$e + A^+ \Leftrightarrow \epsilon_\lambda + \begin{cases} A^* \\ \bar{e} + A^+ \end{cases} \qquad (2)$$

and with the electron–atom free–free (emission/bremsstrahlung) transitions

$$e + A \Leftrightarrow \epsilon_\lambda + \bar{e} + A. \qquad (3)$$

These reactions are generally known to be an important source of continuous emission from plasma and (3) are always taken into account when a partially ionized plasma is considered. If the stable negative ion A^- exists, we shall consider, apart from (3), the electron–atom free–bound radiative processes of photocapture/photodissociation

$$e + A \Leftrightarrow \epsilon_\lambda + A^-. \qquad (4)$$

If reaction (4) occurs as it does in a hydrogen plasma, it usually dominates a relatively weaker channel (3) and therefore cannot be ignored.

2.2. Emission

The partial (a, b) and total (ab) spectral emissivities $\varepsilon^{(a,b)}(\lambda)$ and $\varepsilon^{(ab)}(\lambda) \equiv \varepsilon^{(a)}(\lambda) + \varepsilon^{(b)}(\lambda)$ (per unit volume and wavelength interval, integrated over the emission angle) for the emission ($\Rightarrow$) channels (1*a*,*b*) are related to the spectral coefficients of emission $S^{a,b,ab}$ (per unit atomic and ionic concentrations and per unit wavelength interval) thus

$$\varepsilon^{(a,b,ab)}(\lambda) = S^{(a,b,ab)}(\lambda) N(A) N(A^+) \qquad (5)$$

$$S^{(ab)}(\lambda) = S^{(a)}(\lambda) + S^{(b)}(\lambda), \qquad (6)$$

where $N(A)$, $N(A^+)$ are atomic and ionic densities.

The branching coefficients $X^{a,b}(\lambda)$ for the relative emission yield of channels (1*a*) and (1*b*) are given by

$$X^{(a,b)}(\lambda) = \frac{\varepsilon^{(a,b)}(\lambda)}{\varepsilon^{(ab)}(\lambda)} = \frac{S^{(a,b)}(\lambda)}{S^{(ab)}(\lambda)} \qquad (7)$$

where $X^{(a)} + X^{(b)} = 1$.

For the emission ($\Rightarrow$) channels of electron–ion (2) and electron–atom (3,4) radiative processes, the corresponding quantities are radiation spectral densities $\varepsilon_{ei}(\lambda)$, $\varepsilon_{ea}^{f-f}(\lambda)$ and $\varepsilon_{ea}^{f-b}(\lambda)$ expressed in terms of the spectral coefficients S_{ei}, $S_{ea}^{(f-f)}$, and $S_{ea}^{(f-b)}$ as

$$\varepsilon_{ei}(\lambda) = S_{ei}(\lambda) N(e) N(A^+) \qquad (8)$$

$$\varepsilon_{ea}^{(f-f)}(\lambda) = S_{ea}^{(f-f)}(\lambda) N(e) N(A) \qquad (9)$$

$$\varepsilon_{ea}^{(b-f)}(\lambda) = S_{ea}^{(b-f)}(\lambda) N(e) N(A) \qquad (10)$$

where $N(e)$ is the free-electron density. The superscripts f–f and f–b label the 'free–free' and 'free–bound' electron transitions in the field of the target atom A.

The emissivity ratio F studied in the present work

$$F(\lambda) = \frac{\varepsilon^{(ab)}(\lambda)}{\varepsilon_e(\lambda)} \qquad (11)$$

compares the intensity of the continuous emission from the ion–atom channels with that from the electronic channels (2)–(4). In equation (11), $\varepsilon_e(\lambda) = \varepsilon_{ei}(\lambda) + \varepsilon_{ea}(\lambda)$ where $\varepsilon_{ea}(\lambda) = \varepsilon_{ea}^{ff}(\lambda) + \varepsilon_{ea}^{fb}(\lambda)$ if the stable negative atomic ion A^- exists, and $\varepsilon_{ea}(\lambda) = \varepsilon_{ea}^{ff}(\lambda)$ otherwise. The contribution of molecular continua which is relatively small in the range of T considered, has not been included in ε_e.

2.3. Absorption

For absorption channels (⇐) of ion–atom reactions (1*a,b*) the partial and total absorption coefficients $\kappa^{(a,b)}(\lambda)$, and $\kappa^{(ab)}(\lambda) = \kappa^{(a)}(\lambda) + \kappa^{(b)}(\lambda)$ are

$$\kappa^{(a,b,ab)}(\lambda) = K^{(a,b,ab)}(\lambda)N(\mathrm{A})N(\mathrm{A}^+) \qquad (12)$$

$$K^{(ab)}(\lambda) = K^{(a)}(\lambda) + K^{(b)}(\lambda). \qquad (13)$$

It is assumed for the photodissociative channel (1*a*) that $K^{(a)}N(\mathrm{A})N(\mathrm{A}^+) \equiv K^{(a)}_{\mathrm{pd}}N(\mathrm{A}_2^+)$, where $N(\mathrm{A}_2^+)$ is the molecular ion A_2^+ density, and $K^{(a)}_{\mathrm{pd}}$ is the usual molecular coefficient of absorption due to photodissociation of these ions. Then $K^{(a)} \equiv K^{(a)}_{\mathrm{pd}}N(\mathrm{A}_2^+)/N(\mathrm{A})N(\mathrm{A}^+)$.

Absorption channels (⇐) of the electron–ion (2) and electron–atom (3,4) radiative processes can be described by the spectral absorption coefficients $\kappa_{\mathrm{ei}}(\lambda)$, $\kappa^{\mathrm{ff}}_{\mathrm{ea}}(\lambda)$, $\kappa^{\mathrm{fb}}_{\mathrm{ea}}(\lambda)$.

In local thermodynamic equilibrium (LTE), the absorption ratio $\kappa^{(ab)}/\kappa_{\mathrm{e}}$, where $\kappa_{\mathrm{e}} = \kappa_{\mathrm{ei}} + \kappa^{\mathrm{ff}}_{\mathrm{ea}} + \kappa^{\mathrm{fb}}_{\mathrm{ea}}$, coincides with the emissivity ratio (11) and either can be used to obtain the same estimate for the relative contribution of ion–atom collisions to the radiation processes in the plasma. However, if some of the conditions needed for the LTE are not satisfied, these two ratios are different. In the latter case, more information is required to obtain a quantitative description of absorption in the plasma.

3. General theory

For an arbitrary energy distribution of atomic particles, the spectral coefficients of spontaneous emission $S^{(a,b,ab)}$, equation (6), are defined as

$$S^{(a,b,ab)}(\lambda) = \epsilon_\lambda \left\langle v \frac{\mathrm{d}\sigma^{(a,b,ab)}}{\mathrm{d}\lambda} \right\rangle_{\mathrm{at}} \qquad (14)$$

where $v = \sqrt{2E/\mu_{\mathrm{A}}}$ is the initial relative velocity of A and A^+, and the averaging is taken with the distribution function $f_{\mathrm{at}}(E)$ for the initial kinetic energy E of the complex $\mathrm{A} + \mathrm{A}^+$ measured in the centre-of-mass frame. The distribution f_{at} satisfies the normalization condition

$$\int_0^\infty f_{\mathrm{at}}(E)E^{1/2}\,\mathrm{d}E = 1. \qquad (15)$$

For *thermal* velocities v considered here, the differential (in λ) cross sections $\mathrm{d}\sigma^{a,b,ab}/\mathrm{d}\lambda$, for continuous radiation in (1*a,b*), can be obtained from the quasistatic molecular model of the semiclassical adiabatic approximation (Mihajlov and Popović 1981). It is sufficient to consider, at any time t during the $\mathrm{A} + \mathrm{A}^+$ collision, only the two lowest molecular states of A_2^+: the ground $|1\rangle$ and the first excited $|2\rangle$ electronic Σ^+, states, with the corresponding adiabatic molecular terms $U_1(R)$ and $U_2(R)$. These terms, which depend parametrically on the internuclear separation $R(t)$, are shown schematically in figure 1. The zero energy is chosen in such a way that $U_{1,2}(R) \to 0$ as $R \to \infty$.

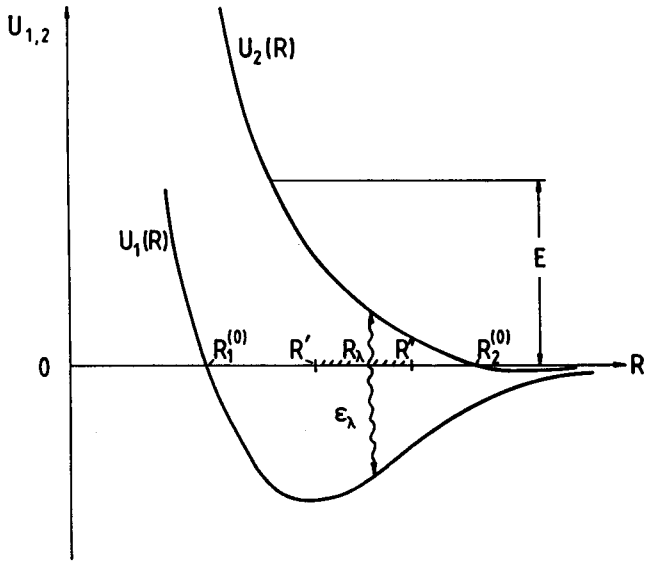

Figure 1. Continuous radiation in $\mathrm{A} + \mathrm{A}^+$ collisions, equations (1*a,b*). The quasistatic model with two adiabatic terms $U_1(R)$ and $U_2(R)$. The validity range for the model is $R_1^{(0)} \leqslant R \leqslant R_2^{(0)}$. A typical range which corresponds to the photon transitions with energy ε_λ considered in the present work is $R' \leqslant R_\lambda \leqslant R''$. Other notations are in the text.

For the total emission processes, the state $|2\rangle$ is initial and the system moves along the repulsive term $U_2(R)$. In the quasistatic approximation, the transition of a photon with wavelength λ and energy ε_λ takes place at a separation R_λ which corresponds to the resonance condition

$$U_2(R) - U_1(R) = \varepsilon_\lambda. \qquad (16)$$

The interval $R' \leqslant R_\lambda \leqslant R''$ which is treated in the present case (see figure 1) corresponds to the near-UV, visible and near-infrared portions of the emission spectrum. The interval is only a part of the total validity range $R_1^{(0)} \leqslant R_\lambda \leqslant R_2^{(0)}$, where the two-channel quasistatic model is applicable.

In the quasistatic approximation, the differential cross section $\mathrm{d}\sigma^{(ab)}/\mathrm{d}\lambda$ for the total process *ab* which includes both photoassociation/dissociation *a* and photocapture *b*, is given by

$$\frac{\mathrm{d}\sigma^{(ab)}(\lambda, E)}{\mathrm{d}\lambda} = P_{\mathrm{i}} \frac{64\sqrt{2}\pi^3\mu_{\mathrm{A}}^{1/2}R_\lambda^2 D_{12}^2(R_\lambda)}{3\hbar\lambda^4\gamma(R_\lambda)} E^{-1} \times \begin{cases} 0 & E < U_2(R_\lambda) \\ (E - U_2(R_\lambda))^{1/2} & E \geqslant U_2(R_\lambda) \end{cases} \qquad (17)$$

where $P_{\mathrm{i}} = 1/2$ is the probability for the system $\mathrm{A}+\mathrm{A}^+$ to be initially in the state $|2\rangle$; the dipole matrix element $D_{12} = \langle 1|\mathbf{D}|2\rangle$; and the logarithmic derivative $\gamma(R_\lambda)$ in equation (17) is given by

$$\gamma(R_\lambda) = |\mathrm{d}\ln[(U_2(R) - U_1(R))/2Ry]/\mathrm{d}(R/a_0)|_{R=R_\lambda}. \qquad (18)$$

Then the total emission coefficient $S^{ab}(\lambda)$ in the quasistatic approximation takes the form

$$S^{(ab)}(\lambda) = \frac{128\pi^4 c}{3} \frac{R_\lambda^2 D_{12}^2(\lambda)}{\lambda^5\gamma(R_\lambda)} W(U_2(R_\lambda)) \qquad (19)$$

Table 1. Parameters R_λ, $U_2(R_\lambda)$ (in au), and C_λ of molecular ions H_2^+ and He_2^+, used in the present calculations of spectral emission $S^{(ab)}$, for $100 \leqslant \lambda$ (nm) $\leqslant 1000$.

	H			He		
	$\gamma_H = 1$			$\gamma_{He} = 1.345$		
λ (nm)	R_λ	$U_2(R_\lambda)$	$C(R_\lambda)$	R_λ	$U_2(R_\lambda)$	$C(R_\lambda)$
100	1.91	0.3645	0.677	1.87	0.3764	1.092
150	2.46	0.2141	0.784	2.20	0.2205	1.052
200	2.86	0.1491	0.838	2.43	0.1523	1.037
250	3.17	0.1141	0.875	2.62	0.1150	1.029
300	3.42	0.0917	0.901	2.77	0.0918	1.025
400	3.81	0.0647	0.939	3.01	0.0649	1.020
500	4.12	0.0492	0.966	3.19	0.0499	1.018
600	4.37	0.0392	0.987	3.35	0.0404	1.017
700	4.58	0.0324	1.003	3.47	0.0338	1.016
800	4.77	0.0275	1.016	3.58	0.0291	1.016
900	4.93	0.0237	1.027	3.68	0.0255	1.015
1000	5.05	0.0213	0.993	3.77	0.0227	1.015

where the factors at the start of the expression depend only upon the molecular parameters of the colliding system and the distribution function $f_{at}(E)$ enters the function $W(y)$ given by

$$W(y) = \int_y^\infty (E - U_2(R_\lambda))^{1/2} f_{at}(E)\, dE. \qquad (20)$$

The partial differential cross sections $d\sigma^{(a,b)}/d\lambda$ and partial emission coefficients $S^{(a,b)}$ can be obtained from the total quantities $d\sigma^{(ab)}/d\lambda$ and $S^{(ab)}$, equations (17) and (19), if we note that, as follows from the energy balance at $R = R_\lambda$, channel a is open only at collisional energies $U_2(R_\lambda) \leqslant E < \epsilon_\lambda$, and channel b only at $E \geqslant \epsilon_\lambda$. This determines the integration ranges for a and b, with respect to E, in (20). We have thus

$$S^{(a,b)} = S^{(ab)} X^{(a,b)} \qquad (21)$$

with the branching coefficients

$$X^{(a)} = 1 - X^{(b)} \qquad X^{(b)} = W(\varepsilon_\lambda)/W(U_2(R_\lambda)). \qquad (22)$$

The expressions (19) and (20) are general in that they do not assume any particular form for the distribution function f_{at} and may be applied to an arbitrary (equilibrium or non-equilibrium) state of the plasma. They may be used, for instance, for plasmas with an excessive concentration of fast ions or in the situation where there are several preferable velocity regions in the distribution. Strongly non-equilibrium plasmas have been studied in many experiments to date, for instance in recent experiments on low-pressure discharges in hydrogen (Petrović *et al* 1992) and in argon plasmas in the diffuse glow regime (Vrhovac *et al* 1992).

4. Maxwellian distributions

For a Maxwellian distribution with given temperature T: $f_{at}(E) = (kT)^{-3/2} \exp(-E/kT)/\Gamma(3/2)$, the spectral coefficients become functions of T, $S^{(a,b,ab)}(\lambda) = S^{(a,b,ab)}(\lambda, T)$. Using equation (19), one obtains the total emission coefficient $S^{(ab)}(\lambda, T)$ (expressed in units of J cm^3 s^{-1} nm^{-1}), as follows

$$S^{(ab)}(\lambda, T) = 4.777 \times 10^{-34} \frac{C(R_\lambda)(R_\lambda/a_0)^4}{\gamma_A(1 - \delta_A a_0/R_\lambda)} \left(\frac{\epsilon_\lambda}{2Ry}\right)^5 \times \exp\left(\frac{-U_2(R_\lambda)}{kT}\right) \qquad (23)$$

where

$$C(R_\lambda) = \left[\frac{2D_{12}(R_\lambda)}{eR_\lambda}\right]^2 \frac{\gamma_A(1 - \delta_A a_0/R_\lambda)}{\gamma(R_\lambda)}$$

$$\delta_A = \frac{1}{\gamma_A}\left(\frac{2}{\gamma_A} - 1\right). \qquad (24)$$

In the above equations, $\gamma_A = (I_A/Ry)^{1/2}$ where I_A is the ionization potential of atom A, and $\gamma(R_\lambda)$ is given by relation (18). Then the partial emission coefficients $S^{(a)}(\lambda, T)$ and $S^{(b)}(\lambda, T)$ are obtained according to

$$S^{(a,b)}(\lambda, T) = S^{(ab)}(\lambda, T) X^{(a,b)}(Z) \qquad (25)$$

and

$$X^{(a)}(Z) = 1 - X^{(b)}(Z) \qquad X^{(b)}(Z) = \frac{\Gamma(3/2; Z)}{\Gamma(3/2)} \qquad (26)$$

where $Z = |U_1(R_\lambda)|/kT$ and $\Gamma(3/2; Z)$ is the incomplete gamma function tabulated, for instance, by Abramowitz and Stegun (1972).

The coefficient $C(R_\lambda)$ in equation (23) is close to unity in the visible and near-infrared parts of the spectrum, though it may differ from unity by some 20% or even more in the near-UV (see table 1). Therefore, for crude estimates of the spectral coefficients, $C(R_\lambda)$ can be replaced by 1 in the full range of λ considered, thus avoiding the calculation of the derivative term (18).

Table 2. Hydrogen plasma. Spectral coefficient of spontaneous emission $S^{(ab)}(\lambda, T)$, equation (23) (in units of 10^{-38} J cm^3 s^{-1} nm^{-1}).

λ (nm)	T (K)						
	4000	5000	6000	8000	10000	12000	16000
200	1.95(−2)	2.05(−1)	9.86(−1)	7.02	2.28(+1)	4.99(+1)	1.33(+2)
250	1.51(−1)	9.13(−1)	3.04	1.36(+1)	3.36(+1)	6.12(+1)	1.30(+2)
300	4.83(−1)	2.05	5.39	1.80(+1)	3.71(+1)	6.01(+1)	1.10(+2)
350	9.73(−1)	3.23	7.20	1.96(+1)	3.57(+1)	5.33(+1)	8.80(+1)
400	1.50	4.16	8.21	1.92(+1)	3.20(+1)	4.50(+1)	6.89(+1)
450	1.95	4.72	8.50	1.78(+1)	2.76(+1)	3.71(+1)	5.36(+1)
500	2.27	4.94	8.30	1.58(+1)	2.34(+1)	3.03(+1)	4.18(+1)
550	2.47	4.92	7.79	1.39(+1)	1.96(+1)	2.46(+1)	3.28(+1)
600	2.54	4.72	7.14	1.20(+1)	1.63(+1)	2.01(+1)	2.60(+1)
650	2.53	4.43	6.43	1.03(+1)	1.36(+1)	1.64(+1)	2.07(+1)
700	2.44	4.08	5.74	8.79	1.13(+1)	1.35(+1)	1.67(+1)
750	2.32	3.71	5.08	7.51	9.50	1.11(+1)	1.35(+1)
800	2.17	3.35	4.48	6.43	7.98	9.23	1.11(+1)
900	1.85	2.70	3.46	4.73	5.71	6.47	7.56
1000	1.40	1.96	2.46	3.25	3.85	4.31	4.96

Table 3. Hydrogen plasma. Spectral coefficient of absorption $K^{(ab)}(\lambda, T)$, equation (27) (in units of 10^{-38} cm^5).

λ (nm)	T (K)						
	4000	5000	6000	8000	10000	12000	16000
200	2.69	7.77(−1)	3.40(−1)	1.21(−1)	6.48(−2)	4.28(−2)	2.53(−2)
250	1.74	5.94(−1)	2.90(−1)	1.18(−1)	6.90(−2)	4.80(−2)	3.01(−2)
300	1.26	4.88(−1)	2.59(−1)	1.17(−1)	7.24(−2)	5.22(−2)	3.40(−2)
350	9.92(−1)	4.22(−1)	2.39(−1)	1.17(−1)	7.52(−2)	5.57(−2)	3.72(−2)
400	8.24(−1)	3.78(−1)	2.25(−1)	1.17(−1)	7.78(−2)	5.86(−2)	3.99(−2)
450	7.11(−1)	3.48(−1)	2.15(−1)	1.17(−1)	7.99(−2)	6.11(−2)	4.22(−2)
500	6.32(−1)	3.25(−1)	2.08(−1)	1.17(−1)	8.18(−2)	6.32(−2)	4.40(−2)
600	5.29(−1)	2.95(−1)	1.98(−1)	1.18(−1)	8.48(−2)	6.65(−2)	4.69(−2)
700	4.65(−1)	2.75(−1)	1.92(−1)	1.19(−1)	8.68(−2)	6.87(−2)	4.89(−2)
800	4.22(−1)	2.61(−1)	1.87(−1)	1.19(−1)	8.81(−2)	7.02(−2)	5.03(−2)
900	3.91(−1)	2.50(−1)	1.82(−1)	1.19(−1)	8.89(−2)	7.12(−2)	5.12(−2)
1000	3.32(−1)	2.20(−1)	1.64(−1)	1.10(−1)	8.27(−2)	6.67(−2)	4.83(−2)

Let us further assume that, apart from the Maxwellian distribution $f_{at}(E, T)$, there exists, at the same T, the dissociative–associative equilibrium between components A, A^+ and A_2^+ for given densities $N(A)$ and $N(A^+)$. In the latter case, the spectral absorption coefficients $K^{(a,b,ab)}(\lambda, T)$ may be determined from the principle of thermodynamical balance (Mihajlov and Dimitrijević 1986, 1992). The total absorption coefficient (in units of cm^5) is then given as

$$K^{(ab)}(\lambda, T) = 0.620 \times 10^{-42} \frac{C(R_\lambda)(R_\lambda/a_0)^4}{\gamma_A(1 - \delta_A a_0/R_\lambda)} \times \exp\left(\frac{-U_1(R_\lambda)}{kT}\right)\theta(\lambda, T) \quad (27)$$

where the function $\theta(\lambda, T)$

$$\theta(\lambda, T) = 1 - \exp(\varepsilon_\lambda/kT) \quad (28)$$

accounts for the stimulated emission.

The partial absorption coefficients are obtained from (27) as

$$K^{(a,b)}(\lambda, T) = K^{(ab)}(\lambda, T)X^{(a,b)}(Z) \quad (29)$$

where the branching coefficients $X^{(a,b)}$ are determined by equations (26).

Finally, we note that the assumptions introduced in this section, are automatically satisfied for an LTE plasma. However, they are weaker than the LTE conditions. Consequently, the theory developed above may be applied in a wider case where LTE does not necessarily exist.

5. Results and discussion

5.1. Atomic and molecular data

Calculations have been carried out for H, He, Li and Na plasmas. For H and He, the atomic parameter γ_A and the

Table 4. Helium plasma. Spectral coefficient of spontaneous emission $S^{(ab)}(\lambda, T)$, equation (23) (in units of 10^{-38} J cm^3 s^{-1} nm^{-1}).

λ	T (K)						
(nm)	4000	6000	8000	10000	12000	16000	20000
200	5.06(−3)	2.78(−1)	2.06	6.87	1.53(+1)	4.17(+1)	7.60(+1)
250	4.21(−2)	8.69(−1)	3.95	9.78	1.79(+1)	3.82(+1)	6.01(+1)
300	1.32(−1)	1.48	4.95	1.02(+1)	1.66(+1)	3.04(+1)	4.36(+1)
350	2.52(−1)	1.87	5.10	9.30	1.39(+1)	2.29(+1)	3.10(+1)
400	3.66(−1)	2.02	4.74	7.91	1.11(+1)	1.71(+1)	2.20(+1)
450	4.50(−1)	1.99	4.17	6.51	8.77	1.27(+1)	1.59(+1)
500	4.98(−1)	1.85	3.57	5.29	6.87	9.54	1.16(+1)
550	5.15(−1)	1.67	3.00	4.27	5.40	7.24	8.64
600	5.10(−1)	1.47	2.51	3.45	4.27	5.56	6.52
650	4.89(−1)	1.29	2.09	2.80	3.39	4.32	5.00
700	4.59(−1)	1.12	1.74	2.28	2.72	3.40	3.89
750	4.24(−1)	9.65(−1)	1.46	1.87	2.20	2.70	3.06
800	3.88(−1)	8.33(−1)	1.22	1.54	1.79	2.17	2.43
900	3.18(−1)	6.22(−1)	8.70(−1)	1.06	1.22	1.44	1.59
1000	2.58(−1)	4.68(−1)	6.30(−1)	7.53(−1)	8.49(−1)	9.85(−1)	1.08

Table 5. Helium plasma. Spectral coefficient of absorption $K^{(ab)}(\lambda, T)$, equation (27) (in units of 10^{-38} cm^5).

λ	T (K)						
(nm)	4000	6000	8000	10000	12000	16000	20000
200	7.00(−1)	9.59(−2)	3.55(−2)	1.95(−2)	1.31(−2)	7.90(−3)	5.77(−3)
250	4.87(−1)	8.31(−2)	3.43(−2)	2.01(−2)	1.40(−2)	8.85(−3)	6.58(−3)
300	3.45(−1)	7.11(−2)	3.22(−2)	1.99(−2)	1.44(−2)	9.38(−3)	7.08(−3)
350	2.57(−1)	6.20(−2)	3.03(−2)	1.96(−2)	1.45(−2)	9.70(−3)	7.40(−3)
400	2.01(−1)	5.53(−2)	2.88(−2)	1.92(−2)	1.45(−2)	9.89(−3)	7.60(−3)
450	1.64(−1)	5.02(−2)	2.75(−2)	1.88(−2)	1.44(−2)	9.99(−3)	7.73(−3)
500	1.38(−1)	4.64(−2)	2.64(−2)	1.85(−2)	1.44(−2)	1.00(−2)	7.80(−3)
600	1.06(−1)	4.09(−2)	2.48(−2)	1.79(−2)	1.41(−2)	1.00(−2)	7.85(−3)
700	8.73(−2)	3.73(−2)	2.36(−2)	1.74(−2)	1.39(−2)	9.98(−3)	7.83(−3)
800	7.53(−2)	3.47(−2)	2.27(−2)	1.70(−2)	1.36(−2)	9.87(−3)	7.77(−3)
900	6.71(−2)	3.28(−2)	2.19(−2)	1.66(−2)	1.34(−2)	9.74(−3)	7.68(−3)
1000	6.11(−2)	3.13(−2)	2.12(−2)	1.62(−2)	1.31(−2)	9.60(−3)	7.58(−3)

molecular parameters R_λ, $U_2(R_\lambda)$ and $C(R_\lambda)$ required for calculations of $S^{(ab)}$, $K^{(ab)}$ and $X^{(b)}$ are presented in table 1, for λ in the range $100 \leqslant \lambda$ (nm) $\leqslant 1000$. The atomic parameters are $\gamma_{Li} = 0.630$ and $\gamma_{Na} = 0.626$. The molecular parameters R_λ and $U_2(R_\lambda)$ have been obtained from the molecular-ion potential curves $U_1(R)$ and $U_2(R)$ of Madsen and Peek (1971) for H_2^+, Gupta and Madsen (1967) for He_2^+, and Kirby-Docken *et al* (1976) for Li_2^+ and Na_2^+. In the case of H_2^+, the dipole matrix element $D_{12}(R_\lambda)$ which enters equation (24) for $C(R_\lambda)$, has been obtained by a (spline) interpolation of the data from Ramaker and Peek (1973). For He_2^+, D_{12} has been obtained from the asymptotic expression (see Ermolaev and Mihajlov 1991)

$$D_{12}(R_\lambda) = \frac{eR_\lambda}{2} \frac{1 - 0.695(a_0/R_\lambda)^3}{(1 - s^2(R_\lambda))^{1/2}} \qquad (30)$$

where $s(R_\lambda) = [1 + \gamma_{He}R_\lambda/a_0 + (\gamma_{He}R_\lambda/a_0)^2/3]\exp(-\gamma_{He}R_\lambda/a_0)$ is the molecular overlap. In our calculations of $D_{12}(R_\lambda)$ for Li_2^+ and Na_2^+, the interpolated values of oscillator strengths of Kirby-Docken *et al* (1976) have been used.

5.2. Spectral coefficients $S^{(ab)}$ and $K^{(ab)}$

The spectral coefficients $S^{(ab)}(\lambda, T)$ and $K^{(ab)}(\lambda, T)$ have been computed from the general expressions (23) and (27). The calculations for hydrogen and helium plasmas are in the range of $200 \leqslant \lambda$ (nm) $\leqslant 1000$. For the hydrogen plasma, the results are presented in tables 2 and 3, and for the helium plasma in tables 4 and 5. For hydrogen plasma, the present range of T, $4000 \leqslant T$ (K) $\leqslant 16000$, is wider than that ($T \geqslant 8000$ K) considered by Roberts and Voigt (1971). The range $4000 \leqslant T$ (K) $\leqslant 8000$ has not been studied before in hydrogen plasmas. For helium plasma, the temperature range is $4000 \leqslant T$ (K) $\leqslant 20000$. The computed emission coefficients $S^{(ab)}$ show for both H and He that in the present range of λ the dependence on T is particularly strong in the UV part of the spectrum. As T grows, the maximum of $S^{(ab)}$ gradually shifts from

Table 6. Branching coefficients $X^{(b)}(\lambda, T)$, equation (26), for hydrogen and helium plasmas; $\lambda = 400$ nm.

	T (K)						
	4000	6000	8000	10000	12000	16000	20000
H	0.051	0.101	0.159	0.274	0.375	0.459	0.584
He	0.055	0.166	0.283	0.384	0.468	0.592	0.677

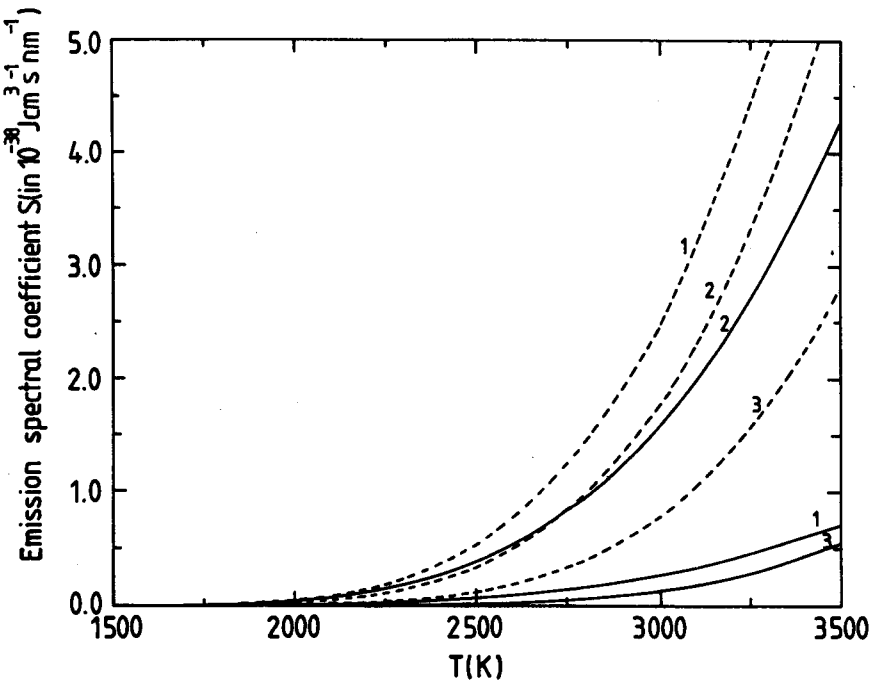

Figure 2. Spectral coefficients $S^{(ab)}(\lambda, T)$ of spontaneous emission (1*a*,*b*) for hydrogen and some alkali metal (Li and Na) plasmas, as a function of T at $\lambda = 400$ nm. These are compared with the corresponding spectral coefficients $S^{f-b}(\lambda, T)$ for radiative capture in the negative ion, equation (4). 1, H; 2, Li; and 3, Na. Full curves, S^{ab}, present work, equation (23); broken curves, S^{f-b} (free–bound transitions) from Armstrong (1963).

the visible region towards the UV. We note that the earlier estimates of ion–atom contribution in helium plasmas (Mihajlov *et al* 1993b) used values of $S^{(ab)}$ which agree within some 10–20% with the more accurate data of the present work where the dipole matrix element was obtained from equation (30).

The semiclassical absorption coefficient $K^{(ab)}$ in both plasmas shows a rapid change with T in the UV part of the spectrum. The strongest dependence of $K^{(ab)}$ on λ is at the lower end of T. For higher plasma temperatures ($T \geqslant 8000$ K for H, and $T \geqslant 10000$ K for He), absorption is practically independent of λ.

In the ranges of λ and T presently considered, our semiclassical photoabsorption data on H_2^+ and He_2^+ can be directly compared with the recent extensive quantum-mechanical calculations of Stancil *et al* (1993) and Stancil (1994) for astrophysical plasmas. The comparison with our earlier calculations (Mihajlov and Dimitrijević 1986, 1992) also shows the importance of the presently implemented accurate interpolation of the molecular parameters $U_2(R_\lambda)$ and $D_{12}(R_\lambda)$. The semiclassical model, despite its simplicity, is adequate within the present ranges of λ and T. For shorter wavelengths ($\lambda < 200$ nm) and lower temperatures ($T < 4000$ K), the quantum-mechanical treatment of Stancil (1994) is expected to give a significant improvement on the semiclassical photoabsorption data.

The branching coefficients $X^{(b)}$ for H and He are displayed in table 6, for a representative value of wavelength $\lambda = 400$ nm, in the temperature range $4000 \leqslant T$ (K) $\leqslant 20000$. Table 6 shows that both species, H and He, produce a similar temperature dependence of the coefficient: a complete domination of the photoassociation channel (1*a*) at the lower end of the temperature range (4000 K), which gradually changes to an equal contribution of both channels (1) at 12000–16000 K. For higher temperatures (20000 K), the radiative charge exchange (1*b*) contributes some 60–70% to the total emission of both ion–atom channels.

For the alkali metal plasmas with relatively low potential of ionization, the range of low temperatures is practically important. The calculations of the emission

coefficient $S^{(ab)}$ in the case of Li and Na have been carried out in the range $1500 \leqslant T$ (K) $\leqslant 3500$, for the visible part of the spectrum. In figure 2 these coefficients are displayed as a function of T (at $\lambda = 400$ nm).

5.3. Comparison of the A_2^+ and $A^+ + A$ continua

The relative contribution of ion–atom collisions (the A_2^+ continuum) to plasma emission can be assessed by considering the emissivity ratio $F(\lambda, T)$, equation (11). This ratio compares the ion–atom contribution with the 'background' electron–ion/atom emission (the A^+ and A continua). The ratio $F(\lambda, T)$ depends, apart from S_{ia}, on the composition of the plasma as well as on the emission coefficients S_{ei} and S_{ea} for the electronic radiative processes (2)–(4).

The concentrations N(e), N(A) and $N(A^+)$ for H and He have been obtained from the Saha equation and the neutrality condition, for each T and p (hydrodynamical pressure). In the case of the hydrogen plasma, an equation analogous to the Saha for N(e), N(H) and $N(H^-)$ has also been used to calculate the concentration of the negative ions H^-. The relative error due to the omission of the molecular component (such as A_2) in these calculations is of the order of $N(A_2^+)/N(A^+)$ and it is generally small, particularly for He ($\leqslant 10\%$), within the full range of T considered. However, it is somewhat higher for the hydrogen plasma at lower T where we have used the corresponding data on N(e), N(H), $N(H^+)$ and $N(H^-)$ from Patch (1969) who had included H_2 in his calculations on the composition of hydrogen plasma. (For hydrogen plasmas above 6000 K, both calculations give concentrations which are practically the same.)

For S_{ei} which include the total contribution of all channels of electron–ion reaction (2), the quasiclassical approximation of Sobelman (1979) was used. The emission coefficients $S_{ea}^{(f-f)}$ for H were obtained from the tabulated data of Stilley and Callawey (1970) and from an analytical approximation of Firsov and Chibisov (1960); for He, we used the tabulated data of Bell *et al* (1982) as well as that of Firsov and Chibisov (1960). The data on $S_{ea}^{(f-b)}$ for H^- were obtained from the tables of Wishart (1979) and from the analytical approximation of Armstrong (1963).

The emissivity ratio $F(\lambda, T)$ reported here has been obtained for the thermal equilibrium where the Maxwellian distributions with the same temperature T are assumed for both free electrons and atomic particles.

In figure 3, the emissivity ratio F is displayed as a function of T, at a representative hydrodynamical pressure p of 1 atm. The cases of H and He are remarkably different from each other owing to the dominating photocapture in hydrogen plasma (4). As figure 3 shows in the full range of T, the emissivity ratio F for the helium plasma, where reaction (4) does not take place, is larger by an order of magnitude than that for the hydrogen plasma. In both cases, F rapidly decays with temperature because of the electron–ion radiative processes which prevail at high T. Nevertheless, even in the case of hydrogen plasma, F is in the range of 0.10–0.15 at intermediate T.

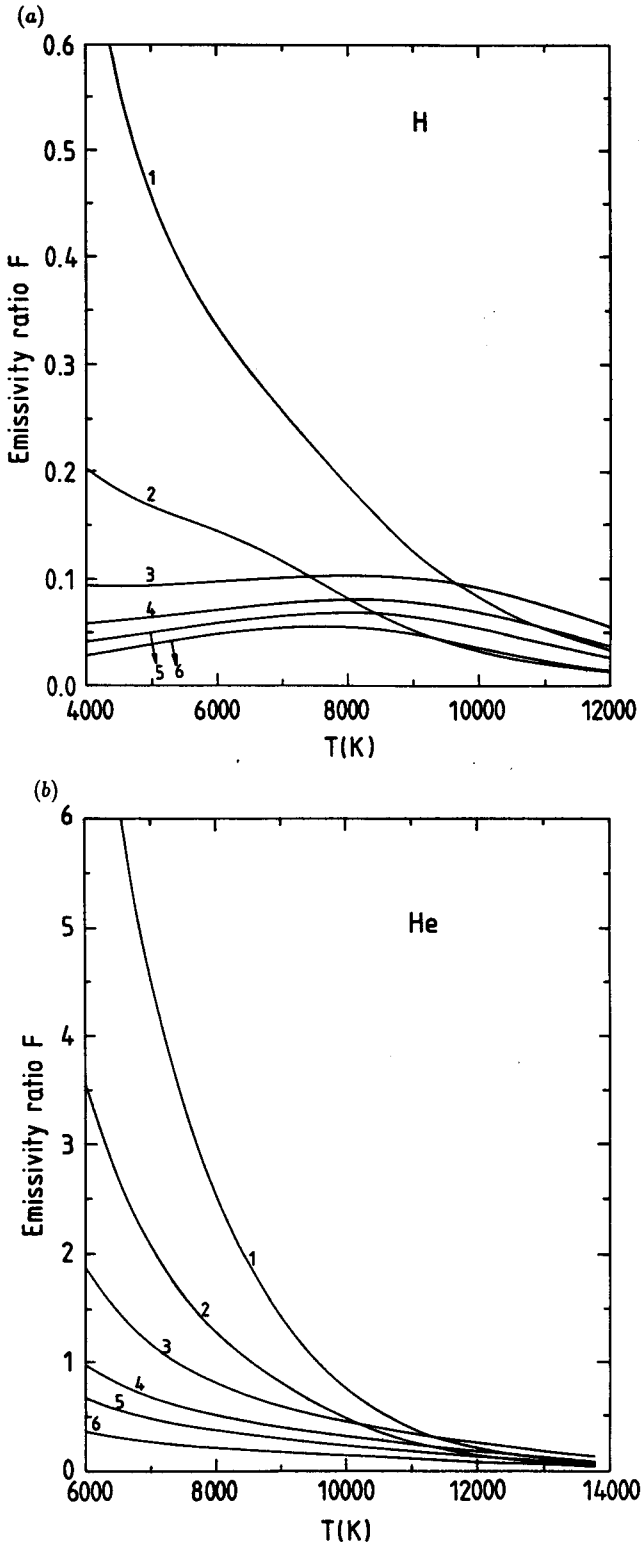

Figure 3. Comparison of the contribution from ion–atom processes (1*a*) and (1*b*) to continuous plasma emission, with that due to electron–ion/atom processes (2)–(4). The emissivity ratio $F(\lambda; p, T)$, equations (11), (5) and (23) for an LTE plasma, as a function of T at constant hydrodynamical pressure, $p = 1$ atm. Wavelength λ: 1, 200 nm; 2, 300 nm; 3, 400 nm; 4, 500 nm; 5, 600 nm; and 6, 800 nm. (*a*) Hydrogen plasma, $\varepsilon_{ea} = \varepsilon_{ea}^{f-f} + \varepsilon_{ea}^{f-b}$. (*b*) Helium plasma, $\varepsilon_{ea} = \varepsilon_{a}^{f-f}$.

Table 7. Comparison of the spectral emissivities for hydrogen plasma computed for $p = 1$ atm and $T = 8000$ K. $\varepsilon_{ia}(\lambda, T)$ are from the present work, equation (5), with $N(H)$ and $N(H^+)$ taken from Patch (1969), and $\varepsilon_{ia}^{RV}(\lambda, T)$ are from Roberts and Voigt (1971). (All emissivities are in units of J cm^{-3} s^{-1} nm^{-1}.)

λ (nm)	ε_{ia}	ε_{ia}^{RV}
100	1.90(−7)	3.46(−7)
150	2.44(−5)	3.05(−5)
200	1.34(−4)	1.54(−4)
250	2.59(−4)	2.95(−4)
300	3.43(−4)	3.73(−4)
350	3.74(−4)	3.80(−4)
550	2.65(−4)	2.50(−4)
600	2.29(−4)	2.08(−4)
650	1.97(−4)	1.78(−4)
700	1.68(−4)	1.50(−4)
800	1.23(−4)	1.06(−4)
900	9.02(−5)	7.67(−5)
1000	6.20(−5)	5.63(−5)

For alkali metal plasmas of Li and Ne, the comparison with ion–atom emission is illustrated in figure 2 only for the spontaneous emission due to photocapture (4). The latter has been obtained from data of Armstrong (1963). Figure 2 displays $S^{(ab)}$ and $S_{ea}^{(f-b)}$ curves for Li and Na as well as for H plasmas.

The comparison between the $S^{(ab)}$ and $S_{ea}^{(f-b)}$ curves for the Na plasma shows that an insignificant contribution from ion–atom reactions (1*a*,*b*) to electronic reactions (4) is expected. However, for the Li plasma the present calculations suggest a noticeable increase in the ion–atom contribution. The variations in the temperature dependence of $S^{(ab)}$, between the Li and Na plasmas, are currently attributed to variations in the molecular parameters R_λ, $U_{1,2}(R)$ and $C(\lambda)$ for these two alkali metals. If the present results are confirmed by more detailed studies (which are intended to include the molecular component of the plasma) then they may indicate a particular importance of ion–atom collisions in the Li plasma.

The present calculations of $\varepsilon_{ia}(\lambda, T)$ (equation (5)) may be compared, for $p = 1$ atm and $T = 8000$ K, with the earlier results of Roberts and Voigt (1971) who used some approximations in the adiabatic model. Table 7 presents both calculations in the range of $100 \leqslant \lambda$ (nm) $\leqslant 1000$. In the visible part of the spectrum, the calculations agree with each other to within 10%. However, the difference grows somewhat larger in the VUV ($\lambda \leqslant 200$ nm).

5.4. Dependence of the emissivity ratio F on λ

As seen in figure 3, the ion–atom contribution is considerably larger in the UV than in the visible part of the spectrum. This can be readily understood if we note that

$$F(\lambda, T) = \varepsilon_{ia}/\varepsilon_e \sim \exp(\varepsilon_\lambda - U_2(R_\lambda)/kT) = \exp(|U_1(R_\lambda)|/kT) \tag{31}$$

where the pre-exponential factor, which depends relatively weakly on λ and T, has been replaced by 1. In the domain of wavelengths $200 \leqslant \lambda$ (nm) $\leqslant 1000$, the term $|U_1(R_\lambda)|$ monotonically grows as λ decreases, as can be seen in figure 1. This causes a rapid (exponential) increase in the F given by equation (31), in the UV part of the spectrum. However, for shorter λ, which have not been considered in the present work, equation (31) predicts a reversed change.

The strong dependence of F on λ is clearly seen in figure 3 at the lower T where the electron–ion emissivity ε_{ei} is small compared with the electron–atom emissivity ε_{ea}. At higher T, the term ε_{ei} is the largest in ε_e and the simple expression (31) which disregards it is not sufficient. Generally, ε_{ei} is a sum of contributions from the photorecombination continua (electronic transitions from the continuum to bound states $A^*(n)$) and, therefore, it is discontinuous, with respect to λ, at thresholds λ_n. The effect of the $n = 2$ threshold is clearly seen in figure 2 for both H and He. In the case of hydrogen, there exists a single threshold at $\lambda_2 = 364.70$ nm whereas for He there are *four* thresholds ($2^{1,3}S$ and $2^{1,3}P$) all lying in the interval $260.18 \leqslant \lambda_2$ (nm) $\leqslant 368.05$. The curves $F(\lambda)$ are split into two distinct families depending on whether the $n = 2$ continuum is included ($\lambda \leqslant \lambda_2$) or excluded ($\lambda > \lambda_2$). Curves 1 (200 nm) and 2 (300 nm) move *below* curve 3 (400 nm) as T increases.

5.5. Dependence of the emissivity ratio F on pressure

Figure 4 presents the emissivity ratio F as a function of T, for a set of hydrodynamical pressures p from 10^{-4} to 10 atm at $\lambda = 400$ nm. As in figure 3, the difference in the magnitude of F between H and He is due to photocapture (4) in the hydrogen plasma.

The dependence of F on pressure is due to the dependence of the emissivities on the concentrations $N(A)$, $N(A^+)$ and $N(\bar{e})$. In order to demonstrate this, let us consider the case of a weakly non-ideal and weakly ionized plasma where the Saha equation can be used. Assuming Maxwellian distributions with the same temperature T for all constituents of the plasma, it is readily shown that

$$F(\lambda, T, p) = \frac{\sqrt{p}}{a_1\sqrt{p} + a_0}. \tag{32}$$

In equation (32) the coefficients $a_1 = (S_{ea}/S_{ia})$ and $a_0 = (S_{ei}/S_{ia})\sqrt{f_{Saha}kT}$, where f_{Saha} is the Saha function and S_{ea} is either $S_{ea}^{(f-f)} + S_{ea}^{(b-f)}$ or $S_{ea}^{(f-f)}$, depending on whether the stable negative ion A^- exists or not.

For lower temperatures, the Saha term in (32) can be neglected and F tends, at any p, to the same limit $1/a_1$

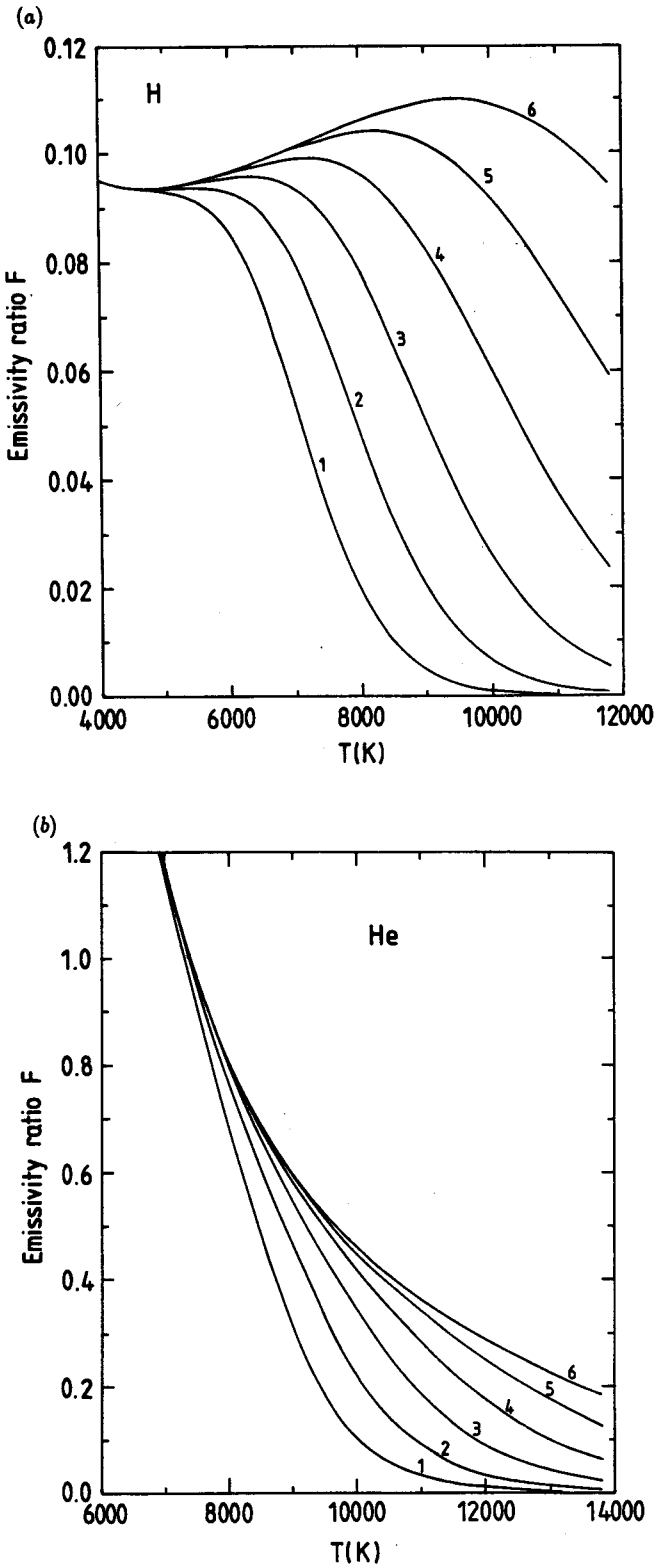

Figure 4. The emissivity ratio $F(\lambda; p, T)$, equations (11), (5) and (23) for an LTE plasma as a function of that at constant wavelength λ = 400 nm. Hydrodynamical pressure p: 1, 10^{-4} atm; 2, 10^{-3} atm; 3, 10^{-2} atm; 4, 10^{-1} atm; 5, 1 atm; and 6, 10 atm. (*a*) Hydrogen plasma. (*b*) Helium plasma.

as T decreases. The independence of F on p at lower T is clearly seen in figure 4 for both H and He. For higher temperatures in the range considered, the Saha term dominates and, for any fixed p, F first decreases exponentially as T increases. At intermediate T, the behaviour of $F(T)$ for hydrogen plasma at different pressures, is complicated by the additional, 'bound–free' term entering S_{ea}. As figure 4 shows, the present calculations demonstrate that in the intermediate range of T the ion–atom contribution to the emission varies significantly with p. This should be taken into account in studies of the ion–atom processes (1*a*,*b*) in the laboratory plasma.

The results presented in figures 3 and 4 suggest that, under certain conditions attainable in laboratory plasmas, the ion–atom contribution to the continuous emission from hydrogen plasma has to be generally treated as a correction. However, in the case of helium laboratory plasmas, this contribution may be significant, or even prevailing.

5.6. The non-equilibrium plasma

One can further consider the case of a strongly non-equilibrium helium plasma. For instance, in the experiments on helium plasma with $N(He^+) \approx N(e)$ described by Aleksandrov *et al* (1969, 1974), the typical atomic temperature T_a was 4500 K and the electronic temperature T_e was 18 000 K. Under such conditions, the e–He collisions play a major role and the $He+He^+$ contribution to the continuous emission is only of the order of 1%. However, with T_a increasing to 8000–13 000 K and with T_e simultaneously approaching T_a, the conditions may arise where an equal contribution to the emission is expected to come from both processes, firstly in the UV and VUV regions of the spectrum. For even higher T, the degree of ionization rapidly increases and electron–ion radiative processes take over. This critical temperature for helium plasma is $\sim$ 13 000 K. For the hydrogen plasma, due to the lower ionization potential of H, this critical temperature is $\sim$ 8000 K. A broad range of conditions realized, for instance, in shock waves, in plasmatrons and in the arc of electrodynamical accelerators of macroparticles (rail-gun) as well as in other laboratory plasmas, are expected to include specific ranges of the conditions particularly favourable for the observation of the ion–atom contribution to continuous emission from the plasma. However, the theoretical studies of such non-equilibrium plasmas would require specific information on the distribution functions $f_{at}(E)$ and $f_e(E)$ as well as on the composition of the plasma, for the particular experimental set-up.

6. Conclusions

We have presented a detailed study of the ion–atom continuous emission from weakly ionized H, He and some alkali metal plasmas, at thermal velocities of the atomic (ionic) species. The radiative cross sections for photoassociation and charge transfer required in these calculations, have been obtained from a quasistatic model, within the semiclassical adiabatic theory of radiative symmetrical ion–atom collisions. We note

that the quasistatic two-term model remains valid at temperatures which are much lower than those considered in the present work. However, the intensity of continuous emission rapidly falls off as T decreases and the bulk of the radiative energy loss in plasma is channelled through line and band emission from the molecular component of the plasma. The latter case, however, is not included in the present discussion.

We have applied the theory to the calculation of the spectral coefficients of the continuous emission from the H, He, Li and Na plasmas, in a wide range of physical conditions corresponding to laboratory plasmas. By comparing the intensity of continuous emission due to ion–atom collisions with that owing to electron–ion/atom radiative collisions (emissivity ratio F), we have been able to estimate the relative importance of the ion–atom radiative collisions in the total balance of the continuous plasma radiation, in a wide range of T and p, for the near-UV, visible and near-IR parts of the spectrum. It has been established that, for helium plasma, F may reach a value of 5–7 in the UV region, whereas for hydrogen plasma F is smaller by an order of magnitude. The suppression of F in the case of hydrogen plasma is due to the dominating photocapture into stable atomic negative ions H^-. In this respect, the hydrogen and helium plasmas represent two different optical types of gaseous media. The results obtained for the helium plasma are expected to remain qualitatively valid in the case of other inert gases.

Calculations of emission coefficients for Li and Na plasmas suggest that, under certain conditions, the contribution of ion–atom radiative collisions to the continuous radiation may be significant. We intend to extend the investigation of the alkaline plasmas to computing the emissivity rate F within a model which takes account of the molecular component in the plasma.

The results are presented in the tabular and graphical forms convenient for applications.

Acknowledgments

The visit of A A Mihajlov to the UK was supported by the Ministry of Science, Technology and Development of Yugoslavia.

References

Abramowitz M and Stegun I 1972 *Handbook of Mathematical Functions* (New York: Dover)
Aleksandrov V Y, Gurevich D B, Mihajlov A A and Podmoshenskii I V 1974 *Sov. Phys.–Opt. Spectrosc.* **37** 489
Aleksandrov V Y, Gurevich D B and Podmoshenskii I V 1969 *Sov. Phys.–Opt. Spectrosc.* **26** 36
Armstrong B H 1963 *Phys. Rev.* **131** 1132
Bates D R 1951a *Mon. Not. R. Astron. Soc.* **111** 303
—— 1951b *J. Chem. Phys.* **19** 1122
Bates D R, Ledsham K and Stewart A L 1953 *Phil. Trans. R. Soc.* **246** 215
Bell K L, Berrington K A and Croskery J P 1982 *J. Phys. B: At. Mol. Phys.* **15** 977
Boggess A 1959 *Astrophys. J.* **129** 432
Ermolaev A M and Mihajlov A A 1991 *J. Phys. B: At. Mol. Opt. Phys.* **24** 155
Firsov O B and Chibisov M I 1960 *Sov. Phys.–JETP* **39** 1770
Gupta B K and Madsen F A 1967 *J. Chem. Phys.* **47** 48
Kirby-Docken K, Cerjan C J and Dalgarno A 1976 *Chem. Phys. Lett.* **40** 205
Madsen M M and Peek J M 1971 *At. Data* **2** 171
Mihajlov A A and Dimitrijević M S 1986 *Astron. Astrophys.* **155** 319
—— 1992 *Astron. Astrophys.* **256** 305
Mihajlov A A, Dimitrijević M S and Ignjatović Lj 1993a *Astron. Astrophys.* **276** 187
—— 1994 *Astron. Astrophys.* **287** 1026
Mihajlov A A, Ermolaev A M and Dimitrijević M S 1993b *J. Quant. Spectrosc. Radiat. Transfer* **50** 227
Mihajlov A A and Popović 1981 *Phys. Rev.* A **23** 1679
Ott W R, Behringer K and Gieres G 1975 *Appl. Opt.* **14** 2121
Ott W R, Fieffe-Prevost P and Wiese W L 1973 *Appl. Opt.* **12** 1618
Patch R W 1969 *J. Quant. Spectrosc. Radiat. Transfer* **9** 63
Petrović Z Lj, Jelenković B M and Phelps A V 1992 *Phys. Rev. Lett.* **68** 325
Ramaker D E and Peek J M 1973 *At. Data* **5** 167
Roberts J R and Voigt P A 1971 *J. Res. NBS* A **75A** 291
Sobelman I I 1979 *Atomic Spectra and Radiative Transitions* (Berlin: Springer) ch 9.5
Stancil P C 1994 *Preprint* 3821, Harvard-Smithsonian Center for Astrophysics
Stancil P C, Bubb J F and Dalgarno A 1993 *Astrophys. J.* **414** 672
Stilley J L and Callawey J 1970 *Astrophys. J.* **160** 245
Vrhovac S B, Radovanov S B, Petrović Z Lj and Jelenković B M 1992 *J. Phys. D: Appl. Phys.* **25** 217
Wishart A W 1979 *Mon. Not. R. Astron. Soc.* **187** 59